22nd International Conference on Sustainable Energy Technologies
Kuala Lumpur, Malaysia, 13 to 15 August 2026 · ISBN 978-1-995850-00-9 · ISSN 2978-4387

CONFERENCE PAPER · ENERGY STORAGE & CONVERSION

Gradient composite structures for suppressing the propagation of thermal runaway in high-capacity $LiFePO_4$ batteries

Chengcheng Zhang[1,2*], Yonghua Yu[1], Kang Qian[2], Zhao Zhang[2], Song Lv[1]

[1] School of Naval Architecture, Ocean and Energy Power Engineering, Wuhan University of Technology, Wuhan, China
[2] China Energy Engineering Group Jiangsu Electric Power Design Institute, Nanjing, China

RECEIVED 26 May 2026 · REVISED 28 June 2026 · ACCEPTED 9 July 2026
PRESENTED 13 to 15 August 2026 · PUBLISHED 23 November 2026

ABSTRACT

High-capacity $LiFePO_4$ batteries are widely used in stationary energy storage systems because of their high energy density and long cycle life. However, thermal runaway may still occur under abusive conditions such as overcharging and overheating. In the tightly packed environment of energy storage systems, thermal runaway can easily lead to large-scale propagation. To enhance the safety of battery systems in energy storage stations, it is crucial to implement reliable and effective measures to suppress thermal runaway propagation. This study established a three-dimensional multi-physics coupled model of a four-cell module composed of 314 Ah prismatic $LiFePO_4$ cells. A symmetric five-layer gradient composite structure consisting of flame-retardant layer | phase-change layer | thermal-insulation layer | phase-change layer | flame-retardant layer was proposed within the 5 mm inter-cell space. The structure was designed to provide thermal shielding, latent-heat absorption, and long-duration thermal insulation, while maintaining bidirectional protection between adjacent cells. Its performance was compared with an unprotected baseline module and several conventional passive suppression strategies, including enhanced convective heat transfer, increased cell spacing, and a 5 mm aerogel insulation layer. The simulations showed that these conventional strategies delayed thermal runaway propagation to different extents but did not prevent subsequent propagation within the investigated period. In contrast, no thermal runaway propagation was observed for the proposed gradient composite structure within the 3000 s simulation window under the specified modelling conditions. These numerical results provide a proof-of-concept and a design reference for passive thermal barriers in high-capacity $LiFePO_4$ modules.

KEYWORDS $LiFePO_4$ batteries, Thermal runaway propagation suppression, Safety enhancement

1. Introduction

Due to their high energy density and long cycle life, $LiFePO_4$ (LFP) batteries are widely used in stationary energy storage systems. According to statistics from the Energy Storage Industry Technology Alliance, as of the end of December 2025, China's cumulative installed capacity for energy storage reached 213.3 GW, a year-on-year increase of 54%. New energy storage technologies, represented by lithium-ion batteries, accounted for more than two-thirds of the installed capacity. The continuously rising demand for energy storage has driven the large-scale application of high-capacity LFP batteries in grid-scale energy storage. Compared to the violent energy release during thermal runaway (TR) in ternary lithium-ion batteries, the inherent safety advantage of LFP batteries stems from the relatively weak oxidising properties of the cathode material; this characteristic is linearly correlated with the intensity of thermochemical reactions within the cell (Zhao *et al.* 2024). However, absolute safety does not exist; LFP batteries can still experience TR under extreme

* Corresponding author. Email address: 2064479452@qq.com (Chengcheng Zhang)

© 2026 The Author(s).
Published by Caravel Press.

doi.org/10.65582/set.2026.013

conditions of abuse. In energy storage stations, a large number of high-capacity cells are densely arranged in modules or clusters. Once a cell experiences TR, the large amount of heat released can rapidly spread to adjacent cells and induce large-scale propagation. The large amount of flammable and explosive gases released during this process can easily trigger fires or even explosions, while toxic gases also pose a threat to human life. Therefore, once a cell's TR becomes uncontrollable, effective containment measures must be implemented to prevent further propagation. Taking into account the economic viability of energy storage stations, space utilisation, and the potential failure of electrical systems during TR, it is more appropriate to adopt passive suppression strategies that occupy minimal space, involve low investment costs, and function reliably–such as filling the gaps between cells with barrier materials.

Numerous studies have investigated TRP suppression in LFP modules, with particular emphasis on inter-cell barrier materials. Ma *et al.* (2023) established a two-dimensional TRP model for modules and investigated the suppression effect of an expanded graphite–paraffin composite phase-change material, finding that this material significantly suppressed TRP under both low and high thermal conductivity conditions. Sun *et al.* (2024) conducted experimental studies on six different thermal insulation materials, finding that a composite phase-change insulation layer achieved zero TRP in packs. Lin *et al.* (2023) developed an inorganic salt hydrate that integrates latent heat storage with thermochemical storage, effectively preventing TRP. Kong *et al.* (2023) inserted mica flakes between cells, delaying TRP by several tens of minutes.

To investigate passive strategies for suppressing TRP in large-format LFP modules, this study established a three-dimensional multiphysics coupled model and proposed a symmetric five-layer gradient composite structure consisting of flame-retardant layer | phase-change layer | thermal-insulation layer | phase-change layer | flame-retardant layer. The total barrier thickness was limited to 5 mm, matching the original inter-cell spacing of the module. The contribution of this structure lies in its discrete functional gradient: the outer flame-retardant layers attenuate the initial thermal and radiative impact, the intermediate phase-change layers absorb transient heat, and the central thermal-insulation layer provides long-duration resistance to heat transfer, while the symmetric arrangement enables bidirectional protection. The proposed configuration was numerically evaluated in a four-cell module composed of 314 Ah prismatic LFP cells and compared with several conventional suppression strategies under identical modelling conditions. No TRP was observed within the 3000 s simulation window for the gradient composite structure. These results provide a numerical proof-of-concept and a design reference for compact passive thermal barriers in high-capacity LFP modules.

2. Mechanisms and characteristics of TR in LFP cells

TR can be triggered when a cell is subjected to external mechanical, electrical, or thermal abuse. In stationary energy storage systems, the likelihood of TR caused by mechanical abuse (such as impact, drops, or puncture) is relatively low; most cases result from overcharging or overheating. Under abusive conditions, the cell temperature continues to rise, and complex physicochemical processes occur internally: first, the SEI film decomposes; this leads to further shrinkage or melting of the separator, causing a short circuit between the cathode and anode; subsequently, the anode reacts violently with the electrolyte; the electrolyte itself also decomposes; finally, the cathode material decomposes, releasing oxygen that reacts with the electrolyte. These chain reactions release a large amount of heat. When the cell's internal heat generation exceeds its ability to dissipate heat to the environment, heat accumulates within the cell, causing the temperature to rise continuously and intensifying the exothermic chemical reactions. When the cell's heat generation reaches an uncontrollable stage, this marks the onset of TR.

During TR in LFP cells, in addition to the abnormal rise in cell temperature caused by heat released from internal reactions, numerous physical changes also occur: voltage fluctuations or sudden drops; rapid increases in the concentrations of flammable and toxic gases such as H_2, CO, and

CH_4; increased aerosol concentrations generated by the decomposition of internal materials and the evaporation of electrolyte; and rising internal pressure due to gas accumulation. When the pressure reaches a certain threshold, the gas breaks through the cell structure and is released into the environment. During TR, LFP cells typically do not directly emit flames; however, the flammable and explosive gases released can easily cause fires or explosions when exposed to open flames or electrical sparks (Jia *et al.* 2024).

3. Passive suppression strategies for TRP

3.1. Numerical treatment of TR heat generation

TR of lithium-ion batteries involves a series of strongly exothermic reactions, including decomposition of the SEI, reactions between the anode and electrolyte, electrolyte decomposition, and decomposition of the cathode material. These reactions interact with each other and lead to rapid heat accumulation inside the cell once TR is initiated.

Since the present study focuses on heat transfer and TRP at the module scale rather than on detailed electrochemical reaction kinetics within a cell, the microscopic exothermic reactions were not resolved separately. Instead, their combined thermal effect was represented by a prescribed transient heat-generation profile using the Thermal Event feature in COMSOL Multiphysics. After a thermal event was activated, the corresponding transient heat source was applied to the affected cell to represent the characteristic rapid heat-release stage associated with TR.

The same thermal-event heat-generation treatment was applied consistently to all comparative cases. Therefore, differences among the investigated cases arose from the corresponding thermal-protection strategies and boundary conditions rather than from changes in the prescribed TR heat source.

3.2. Simulation of passive TR mitigation strategies

A 314 Ah prismatic LFP cell used for stationary energy storage was simulated in this study. The modelled cell had a nominal voltage of 3.2 V, a discharge cut-off voltage of 2.5 V, and a charge cut-off voltage of 3.65 V. The cell dimensions were 175 mm × 72 mm × 207 mm, with an LFP cathode and a conductive graphite anode. The simulated module consisted of four cells connected in series. To reduce model complexity and improve computational efficiency, the cell was treated as a homogeneous equivalent domain, while the anisotropy of thermal conductivity in the in-plane and through-thickness directions was retained. The equivalent physical parameters of the cell (such as density, specific heat capacity, and thermal conductivity) were calculated using the volume-weighted average of each component (cathode, anode, separator, and current collector). The geometric configuration of the module consisted of four cells, positive and negative terminals, and busbars, with a 5 mm gap between cells, as shown in Figure 1.

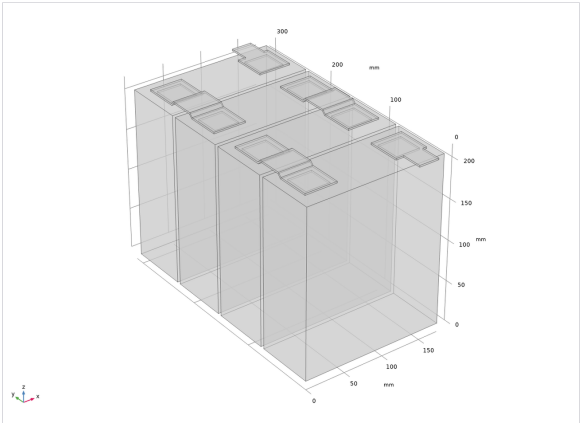

Figure 1. Geometric configuration of the four-cell LFP module.

The second cell from the right was designated as the initially failed cell, as shown in Figure 2, to observe the process of heat transfer to the adjacent cells on both sides. TR was triggered in this cell at 60 s, while the remaining cells were allowed to undergo thermal events when their maximum temperature reached the prescribed activation criterion of 80 °C. Once activated, the transient thermal-event heat source was applied to the corresponding cell. Since TR releases more energy and poses a greater risk of propagation at high SOC levels, the initial SOC of all cells was set to 100% to evaluate the suppression strategies under severe thermal-loading conditions.

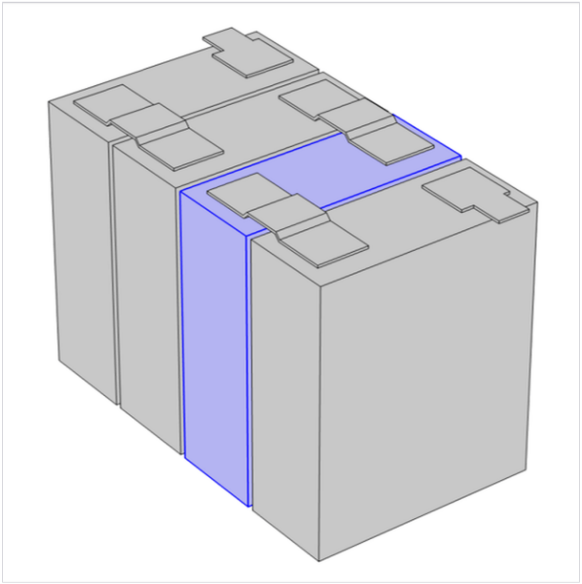

Figure 2. Location of the initially failed cell in the module.

To represent the operating conditions inside the energy storage compartment, the ambient temperature was set to 30 °C. Heat from the cell surface was dissipated into the surrounding environment through two mechanisms: convective heat transfer and radiation. During TR, when the cell temperature is high, radiation becomes the dominant mode of heat transfer, with significant heat being transferred via radiation between the large adjacent surfaces of the cell. Since most LFP cells undergo smouldering rather than spontaneous combustion during TR (Mao *et al.* 2021), the simulation did not include the flame combustion stage. This simulation comprehensively considered the coupled effects of multiple physical fields, including solid-state heat transfer, convective heat transfer, and radiative heat transfer, covering the primary physical processes during TR.

A gradient composite structure was proposed to suppress TRP within the inter-cell gaps of the module. As shown in Figure 3, the composite structure consisted of flame-retardant layer, phase-change layer, and thermal insulation layer. It featured a symmetrical multilayer structure design, with 1-mm-thick flame-retardant and phase-change layers on either side and a 1-mm-thick thermal insulation layer in the middle, resulting in a total thickness of 5 mm. The specific structure was as follows: flame-retardant layer | phase-change layer | thermal insulation layer | phase-change layer | flame-retardant layer. This structure combined multiple functions, including flame retardancy, heat absorption, and thermal insulation.

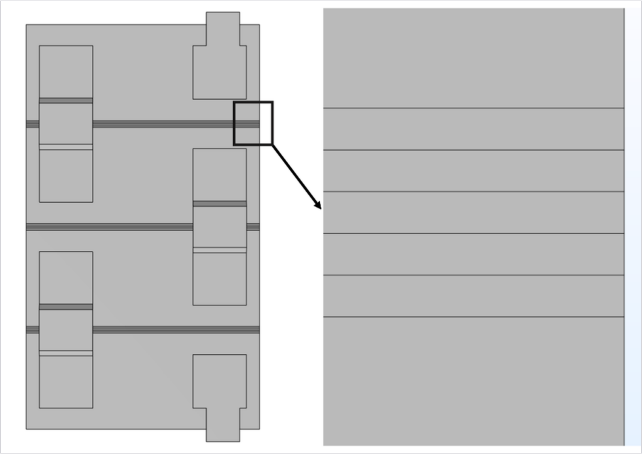

Figure 3. Schematic diagram of a gradient composite structure.

As the first functional barrier in direct contact with the cell surface, the flame-retardant layer is intended to attenuate the initial high-temperature thermal and radiative impact generated during TR. At elevated temperatures, the layer was represented as undergoing endothermic decomposition and formation of a char-like protective state. The resulting porous char structure increases the effective thermal resistance and attenuates heat transfer to adjacent cells. In the numerical model, these effects were represented through equivalent temperature-dependent thermophysical properties rather than explicit chemical reaction kinetics or char-growth processes. The adopted parameters are listed in Table 1.

Table 1. Thermophysical properties of the equivalent functional layers used in the numerical model.

Parameter	Flame-retardant layer	Phase-change layer	Thermal-insulation layer
Thickness / mm	1	1	1
Effective density / kg·m^{-3}	350	1300	250
Effective thermal conductivity / W·m^{-1}·K^{-1}	0.06	0.4	0.02
Effective specific heat / J·kg^{-1}·K^{-1}	1500	2000	1000
Latent heat / kJ·kg^{-1}	—	300	—
Phase-change temperature / °C	—	120	—
Effective phase-change interval / K	—	10	—
Effective decomposition interval / °C	250 - 350	—	—
Effective char-formation temperature / °C	300	—	—
Effective post-char thermal conductivity / W·m^{-1}·K^{-1}	0.05	—	—
Initial emissivity	0.85	—	—
Effective char emissivity	0.9	—	—

The phase-change layer is introduced to provide transient heat absorption through latent-heat storage during the solid–liquid phase transition. When the local temperature reaches the prescribed phase-change range, part of the heat transferred from the TR cell is absorbed as latent heat, thereby reducing the rate of temperature rise on the cold side of the barrier. Research has shown (Zhou *et al.* 2024) that phase-change materials are effective in suppressing TR under both low and high thermal conductivity conditions. In the present numerical study, the PCM was represented by an equivalent set of effective thermophysical parameters rather than by a specific chemical compound. The

corresponding density, thermal conductivity, specific heat capacity, phase-change temperature range, and latent heat used in the model are given in Table 1.

The central thermal-insulation layer is designed to provide long-duration resistance to heat transfer after the transient heat-absorption stage. Its extremely low effective thermal conductivity reduces heat transfer across the inter-cell barrier and limits the thermal load imposed on adjacent cells. In the numerical model, the insulation layer was likewise represented using prescribed equivalent thermophysical properties for evaluating its thermal-insulation function within the multilayer structure. The adopted parameters are summarised in Table 1.

The functional layers were not assigned to specific chemical formulations in the present study. Instead, equivalent thermophysical parameters were adopted to isolate and evaluate the effects of the multilayer functional architecture. Therefore, the present work focuses on structural design rather than material formulation.

To more clearly demonstrate the effectiveness of this gradient composite structure in suppressing TRP, this study also conducted simulations and comparative analyses of other suppression strategies, as shown in Figure 4.

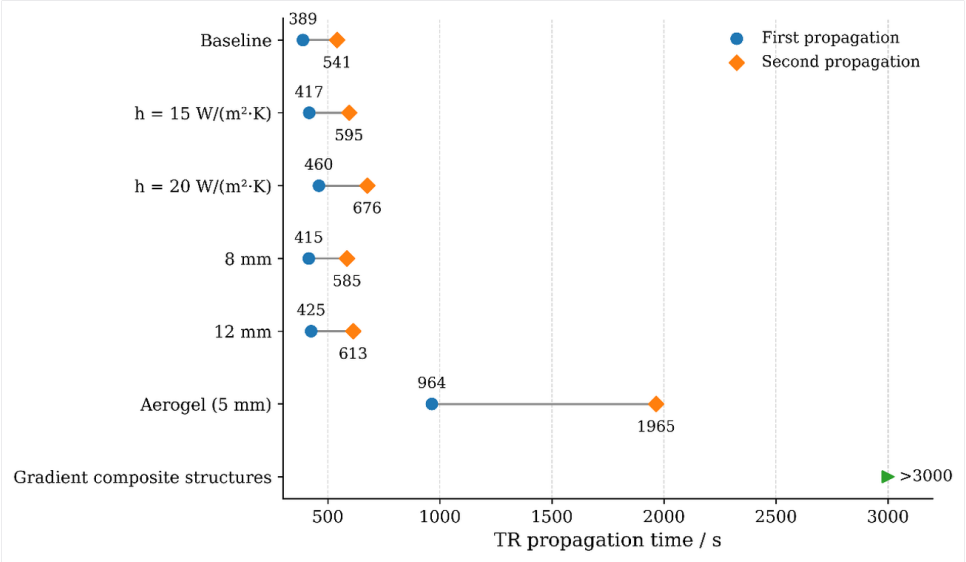

Figure 4. Comparison of the first and second TRP times under different suppression strategies. “>3000” indicates that no TRP was observed within the 3000 s simulation window.

When no measures were taken to suppress TRP in the original module, TR propagated rapidly, as shown in Figure 4. At 389 s, the temperature of the adjacent cell reached 80 °C, triggering TR and resulting in the first instance of TRP.

The convective heat transfer coefficient is a key factor affecting the outward diffusion of heat from the cells. The suppression effects of different convective heat transfer coefficients on TRP are shown in Figure 4. When the convective heat transfer coefficient h = 15 W/(m²·K), the first TRP occurred at 417 s and the second at 595 s; when h = 20 W/(m²·K), the first TRP occurred at 460 s and the second at 676 s. Compared to the baseline model (h = 10 W/(m²·K)), the time to the first TRP was delayed by 28 s and 71 s, respectively, and the time to the second TRP was delayed by 54 s and 135 s, respectively. These results showed that increasing the convective heat transfer coefficient delayed TRP, although the improvement remained limited.

Cell spacing is another factor that influences TRP. As shown in Figure 4, when the cell spacing was increased to 8 mm, the first TRP occurred at 415 s and the second at 585 s; when the cell spacing was 12 mm, the first TRP occurred at 425 s and the second at 613 s. Compared to the original module with a cell spacing of 5 mm, the time to the first TRP was delayed by 26 s and 36 s, respectively, and the

time to the second TRP was delayed by 44 s and 72 s, respectively; increasing the cell spacing also delayed TRP.

When the space between cells was filled with 5 mm of aerogel, the suppression effect on TRP within the module is shown in Figure 4. The first instance of TRP occurred at 964 s and the second at 1965 s. Compared to the original module without any measures, this delayed TRP by 575 s and 1424 s, demonstrating a significant suppression effect.

Overall, the conventional suppression strategies investigated in this study delayed TRP to different extents but did not prevent subsequent propagation within the simulation period. In contrast, no TRP was observed for the gradient composite structure within the 3000 s simulation window under the specified modelling conditions, as shown in Figure 4. The corresponding temperature-field evolution in Figure 5 further shows that the thermal disturbance remained more localised than in the baseline and aerogel cases. These results indicate that the proposed multilayer functional architecture provides stronger suppression of inter-cell heat transfer than the investigated conventional passive strategies.

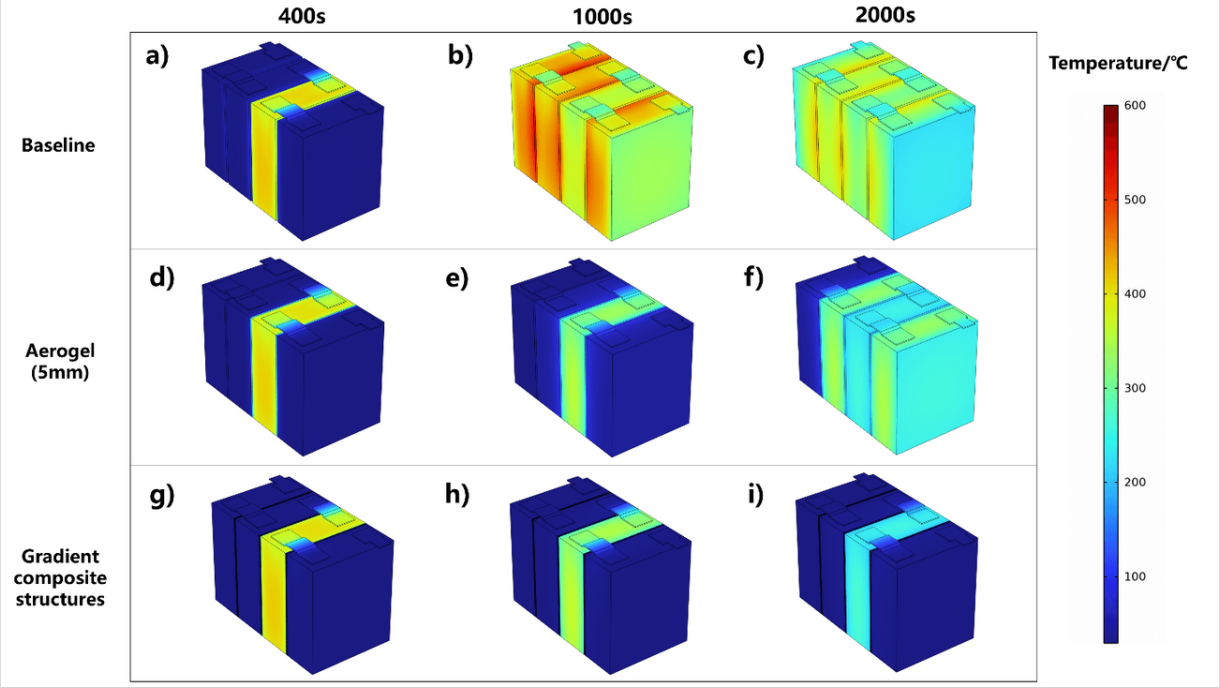

Figure 5. Temperature-field evolution of the four-cell module under representative suppression strategies at selected times: a)-c) baseline, d)-f) Aerogel (5 mm), and g)-i) gradient composite structures at 400 s, 1000 s, and 2000 s, respectively. All subfigures use the same temperature scale for direct comparison.

As shown in Figure 5, distinct differences in heat propagation were observed among the three configurations. At 400 s, shortly after the first TRP in the baseline case, the high-temperature region had begun to extend from the initially failed cell towards the adjacent cells, whereas the thermal influence remained more localised in the aerogel and gradient composite structure cases. At 1000 s, extensive heat propagation was observed in the baseline module, while the aerogel case had just undergone its first TRP event. In contrast, the high-temperature region in the gradient composite structure remained largely confined to the vicinity of the initially failed cell. At 2000 s, heat had propagated through multiple cells in the baseline and aerogel cases, whereas the gradient composite structure continued to restrict the thermal disturbance to a limited region. These temperature-field distributions are consistent with the propagation-time comparison in Figure 4 and further illustrate the ability of the proposed multilayer structure to reduce inter-cell heat transfer under the investigated numerical conditions.

4. Conclusions

As the primary energy storage medium in energy storage stations, large-capacity LFP cells feature high energy density and are deployed in large numbers with dense arrangements. When electrical system failures occur or the cells themselves malfunction, abnormal temperature rises can easily lead to TR. If left uncontrolled, this can rapidly spread throughout the entire cell compartment, triggering large-scale fires and explosions. To suppress TRP and enhance the safety of large-capacity LFP cell systems in energy storage stations, this study proposed the use of a gradient composite structure to passively suppress TRP between cells.

This study established a three-dimensional multi-physics coupled model for high-capacity LFP modules and designed a gradient composite structure that integrates flame retardancy, phase-change heat absorption and thermal insulation functions. Through the triple synergistic effect of "the flame-retardant layer forming char to block radiation, the phase-change layer absorbing latent heat, and the thermal-insulation layer physically blocking heat," no TRP was observed for the proposed structure within the 3000 s simulation window under the specified numerical conditions. Compared with the investigated conventional strategies, the proposed structure provided the longest delay in TRP while retaining the original 5 mm inter-cell spacing. The present study should be regarded as a numerical proof-of-concept, and the proposed configuration has not yet been validated through module-level thermal runaway experiments. Therefore, the numerical results should not be directly extrapolated to practical energy-storage stations without further experimental validation.

Future research should evaluate the structural support capability, cost, service life, and ageing behaviour of the functional layers and should include module-level TRP experiments to validate the proposed architecture. Further optimisation of layer thicknesses, structural configuration, and assembly processes will also be required before practical engineering application.

Declarations

Author contributions. Chengcheng Zhang: Investigation, Formal analysis, Data curation, Writing (original draft), Writing (review and editing), Visualization, Validation, Software. Yonghua Yu: Conceptualization, Methodology. Kang Qian: Supervision, Resources. Zhao Zhang: Project administration. Song Lv: Funding acquisition.

Funding. This research received no specific funding.

Conflicts of interest. The authors declare no competing interests.

Data availability. The data that support the findings of this study are available from the corresponding author upon reasonable request.

References

Jia, Zhuangzhuang; Min, Yuanyuan; Qin, Peng; Mei, Wenxin; Meng, Xiangdong; Jin, Kaiqiang; Sun, Jinhua; Wang, Qingsong (2024) 'Effect of safety valve types on the gas venting behavior and thermal runaway hazard severity of large-format prismatic lithium iron phosphate batteries', *Journal of Energy Chemistry*, 89, pp. 195-207. Available at: https://doi.org/10.1016/j.jechem.2023.09.052

Kong, Qinggang; Qian, Ting; Yan, Yanping; Zhu, Haifeng (2023) 'Thermal Runaway and Propagation Study on $LiFePO_4$ cell in parallel application', *2023 26th International Conference on Electrical Machines and Systems (ICEMS)*. IEEE, pp. 5251-5254. Available at: https://doi.org/10.1109/icems59686.2023.10344925

Lin, Shao; Ling, Ziye; Li, Suimin; Cai, Chuyue; Zhang, Zhengguo; Fang, Xiaoming (2023) 'Mitigation of lithium-ion battery thermal runaway and inhibition of thermal runaway propagation using inorganic salt hydrate with integrated latent heat and thermochemical storage', *Energy*, 266, pp. 126481. Available at: https://doi.org/10.1016/j.energy.2022.126481

Ma, Ruixin; Feng, Xuning; Zhao, Tianyang; Zhang, Wencan; Liu, Min; Wu, Weixiong (2023) 'Composite phase change material for preventing battery thermal runaway propagation: Critical condition and inhibition strategy', *Journal of Energy Storage*, 72, pp. 108237. Available at: https://doi.org/10.1016/j.est.2023.108237

Mao, Binbin; Liu, Chaoqun; Yang, Kai; Li, Shi; Liu, Pengjie; Zhang, Mingjie; Meng, Xiangdong; Gao, Fei; Duan, Qiangling; Wang, Qingsong; Sun, Jinhua (2021) 'Thermal runaway and fire behaviors of a 300 Ah lithium ion battery with $LiFePO_4$

as cathode', *Renewable and Sustainable Energy Reviews*, 139, pp. 110717. Available at: https://doi.org/10.1016/j.rser.2021.110717

Sun, Xiaomei; Dong, Yuanjin; Sun, Peng; Zheng, Bin (2024) 'Effects of thermal insulation layer material on thermal runaway of energy storage lithium battery pack', *Journal of Energy Storage*, 76, pp. 109812. Available at: https://doi.org/10.1016/j.est.2023.109812

Zhao, Liqi; Hou, Junxian; Feng, Xuning; Xu, Jia; Xu, Chengshan; Wang, Huaibin; Liu, Hao; Hou, Bowen; Rui, Xinyu; Gu, Yingzhe; Lu, Languang; Bao, Cheng; Ouyang, Minggao (2024) 'The trade-off characteristic between battery thermal runaway and combustion', *Energy Storage Materials*, 69, pp. 103380. Available at: https://doi.org/10.1016/j.ensm.2024.103380

Zhou, Sili; Lin, Shao; Zhang, Wenbo; Ling, Ziye; Zhang, Zhengguo; Fang, Xiaoming (2024) 'Kinetics study on inhibiting battery thermal runaway using an inorganic phase change material with a super high thermochemical storage capacity', *Process Safety and Environmental Protection*, 191, pp. 643-657. Available at: https://doi.org/10.1016/j.psep.2024.08.134

HOW TO CITE THIS PAPER

Zhang, C., Yu, Y., Qian, K., Zhang, Z. and Lv, S. (2026). Gradient composite structures for suppressing the propagation of thermal runaway in high-capacity $LiFePO_4$ batteries. In: *Proceedings of the 22nd International Conference on Sustainable Energy Technologies (SET2026)*, Kuala Lumpur, Malaysia, 13 to 15 August 2026. Caravel Press, pp. 157–165.
ISBN 978-1-995850-00-9. ISSN 2978-4387. https://doi.org/10.65582/set.2026.013

COPYRIGHT AND LICENCE

© 2026 The Author(s). This is an open access paper distributed under the terms of the Creative Commons Attribution (CC BY 4.0) licence, which permits unrestricted use, distribution and reproduction in any medium, provided the original work is properly cited.

WSSET World Society of Sustainable Energy Technologies Organised by the World Society of Sustainable Energy Technologies. Published by Caravel Press.